Surfaces and Interfaces 22 (2021) 100811

Contents lists available at ScienceDirect

Surfaces and Interfaces

journal homepage: www.sciencedirect.com/journal/surfaces-and-interfaces

Effect of Laser Single Pulse Energy on Micro-structural, Mechanical and Corrosion Properties of Amorphous Ni-Fe-P Alloy Prepared by Laser-Assisted Electrodeposition

Yucheng Wu, Zhaoyang Zhang *, Kun Xu, Jinzhong Lu, Xueren Dai, Hao Zhu, Shuai Yang

Laser Technology Institute, School of Mechanical Engineering, Jiangsu University, Zhenjiang 212013, China

ARTICLE INFO

Keywords:
Amorphous Ni-Fe-P alloy
Laser-assisted electrodeposition
Laser single pulse energy
Properties

ABSTRACT

In this paper, amorphous Ni-Fe-P alloy is prepared by laser-assisted electrodeposition with the manner of laser cyclic scanning. The influence of different laser single pulse energy (12, 14, 16, 18 and 20μJ) on the electrodeposition process and properties of amorphous Ni-Fe-P alloy was studied, including deposition rate, residual internal stress, surface morphology, degree of amorphousness, corrosion resistance, hardness and wear resistance. The results show that with the increase of laser single pulse energy (12~20μJ), the deposition rate has been increasing, which is increased about 50% when the laser single pulse energy is 20μJ compared with no laser irradiation. When the laser single pulse energy is 12~20μJ, the content of P element increased at the beginning and then keep steadily, while the content of Ni elements increases from 12~16μJ and the content of Fe elements increases from 16~20μJ. XRD patterns show that laser irradiation improves the amorphous degree of the coating. When the laser single pulse energy is 16μJ, the residual tensile stress of the coating is 97 Mpa and the surface morphology quality and finish are improved because of the number of pores and cracks is reduced. In addition, corrosion resistance, hardness and wear resistance are the best compared with no laser irradiation when the laser single pulse energy is 16μJ.

1. Introduction

Amorphous Ni-Fe-P alloy is widely used in many fields such as aerospace, medical manufacturing because of good corrosion and wear resistance, etc. [1–4]. Electrodeposition is a normal method used for preparing amorphous alloy, which has many advantages in terms of deposition rate, experimental equipment, processing cost [5–12], however, accompany with some defects such as pores and high residual stress [3,13,14]. Therefore, the method of pure electrodeposition no longer meets the requirements of the industrial field for material performance.

Due to high power and high density, laser processing is used in many fields to improve part performance [15,16]. Some good results have been achieved by many scholars. Zhang et al. [17] observed that the surface morphology and properties of copper were improved by laser-assisted electrodeposition and found that laser thermal effect can refine grains and increase deposition rate. Dai et al. [18] found that the laser irradiation can increase the deposition rate and improve the coating quality due to the increase in solution conductivity and diffusion coefficient caused by laser thermal effect. Yu et al. [19,20] found that laser irradiation can affect the growth direction and grain size in ionic liquid electrodeposition process. Cho et al. [21] deposited a variety of patterns of copper plating successfully on the stainless steel without a mask by the thermal effect of laser. Ramiro et al. [22] used pulsed laser assisted electrodeposition of CdTe and found that the laser pulse energy can improve the structure and optical properties. Jin et al. [23] found that the laser treatment has a beneficial impact for the thermoelectric performances of electrochemically grown semiconductor nanowires. Zouari et al. [24] found that use of a continuous or pulsed laser beam was shown to reduce the P content in the deposit at high current densities and in some cases, amorphous structures were replaced by more crystalline forms with assistance of a laser beam. In summary, laser thermal effects can refine grains and accelerate hydrogen evolution, which is beneficial for the tensile stress reduction and performance of amorphous alloys. However, there are few researches about laser thermal effect on electrodeposited multi-element amorphous alloys, especially amorphous Ni-Fe-P alloy.

In this paper, a laser-assisted electrodeposition composite machining

* Corresponding author.
E-mail address: zzhaoyang@126.com (Z. Zhang).

https://doi.org/10.1016/j.surfin.2020.100811
Received 23 September 2020; Received in revised form 22 October 2020; Accepted 9 November 2020
Available online 14 November 2020

system was conducted to prepare amorphous Ni-Fe-P alloy by laser reciprocating scanning. The laser thermal effect on deposition rate, residual internal stress, surface morphology, degree of amorphousness, corrosion resistance, hardness and wear resistance were discussed. In addition, the mechanism of the laser thermal effect for electrodeposited amorphous Ni-Fe-P alloy were further researched.

2. Experimental details

A laser-assisted electrodeposition processing device mainly including a laser irradiation system and an electrodeposition system is shown in Fig. 1. A picosecond laser micro-machining system (PX1001I-A, Edgewave, Germany) is used in this study. The laser wavelength is 1064nm, the maximum output power is 70W and the frequency range is 0.2~30MHz. The pulse power supply (UTG4082A, Huaqing, China) used in the electrochemical deposition system has a frequency range of 0 to 3000 Hz and a duty ratio of 20% to 100%.

The process conditions for preparing amorphous Ni-Fe-P alloy by hypophosphite system are shown in Table 1.

During the experiment, the laser single pulse energy is changed and other parameters remain unchanged. The samples were polished and then cleaned by ultrasound. Six samples each group were used to compare the difference with or without laser action. Before electrodeposition, the laser power was measured with a power meter (UP19K-110F-H9, Gentec-EO, Canada) and the solution was preheated by irradiation for 10 minutes.

Firstly, a high-precision electronic balance (0.1mg) was used to measure the quality of each sample for five times with three groups to calculated the deposition rate. Secondly, an X-ray stress tester (X-350A, Aisite, China) is used to test residual internal stress. The measurement method is the lateral tilt fixed ψ method. ψ is the crystal plane orientation, which is 0.0°, 25.0°, 35.0°, 45.0°. The peak determination method is cross-correlation. The stress constant is -601 MPa/°, the scanning step (2θ) is 0.10°, the counting time is 0.50s, the high voltage is 22.0KV and the current is 6.0mA. Next, a scanning electron microscope (S-3400, Hitachi, Japan) was used to observe the surface morphology and the attached energy spectrometer (EDS) was used to test the element content with 5 points at least. Then, an X-ray diffractometer (D8 Advance, Bruker, Germany) was used to analyze the degree of amorphous state (35~55°, 5°/min). Then, the full immersion experiment was conducted with 3.5% NaCl (for 144h, 480h) and 2mol/L HCl (for 24h, 72h) solutions to test the corrosion resistance by measuring the sample quality with a high-precision electronic balance (0.1mg) before and after corrosion at least five times. Then, a micro-hardness tester (FM-ARS900, Xinci, China) was used to measure the hardness under a load of 0.98N and a duration of 15s, five points were randomly tested. Then, a wear tester (UMT-2, Bruker, USA) was used to measure wear resistance that the bearing steel is a friction ball, the load is 5N, the reciprocating distance is 5mm, the sliding speed is 50mm/s, and the duration time is 30min. The samples were weighed five times and a scanning electron microscope (JSM-7001F, JEOL, Japan) was used to observe the surface condition after abrasion. Before testing, ensure that the coating thickness is basically the same according to the deposition rate and weight percentage elements.

Table 1
Solution composition and laser parameters.

Parameters	Values
$NiSO_4{\bullet}6H_2O$	120g/L
$FeSO_4{\bullet}7H_2O$	20g/L
$NiCl_2{\bullet}6H_2O$	40g/L
H_3BO_3	40g/L
$Na_3C_6H_5O_7{\bullet}2H_2O$	20g/L
$NaH_2PO_2{\bullet}H_2O$	6g/L
$C_{12}H_{25}OSO_3Na$	0.2g/L
Saccharin	5g/L
PH	2.1-2.2
T	25°C
Anode	Ni (40 × 20 × 2mm) Fe (30 × 15 × 2mm)
Cathode	Cu (10 × 10 × 1.5mm)
Laser current density	$2A/dm^2$
Laser single pulse energy	12~20μJ
Laser frequency	1MHz
Scanning speed	3000mm/s
Scanning line spacing	20μm
Defocus	1mm
Laser diameter	20μm

3. Results and discussion

3.1. Deposition rate

The change in the absorption rate of the solution with the increase in thickness was tested, the results are shown in Fig. 2. As the thickness increases, the absorption rate of the solution also increases. Therefore, considering the cost and absorption rate in this experiment, the thickness of the solution is 15mm. In addition, the absorption rate of the solution under different laser powers was tested. The beaker was placed above the power meter. Keeping the thickness of the solution unchanged and the results are shown in Table 2. The absorption rate of the solution to the laser is about 90%, indicating that the thermal effect of the laser on the solution is significant.

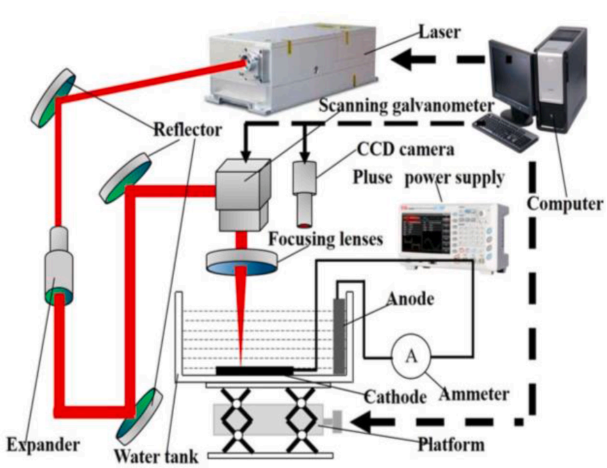

Fig. 1. Schematic diagram of laser electrodeposition composite processing system.

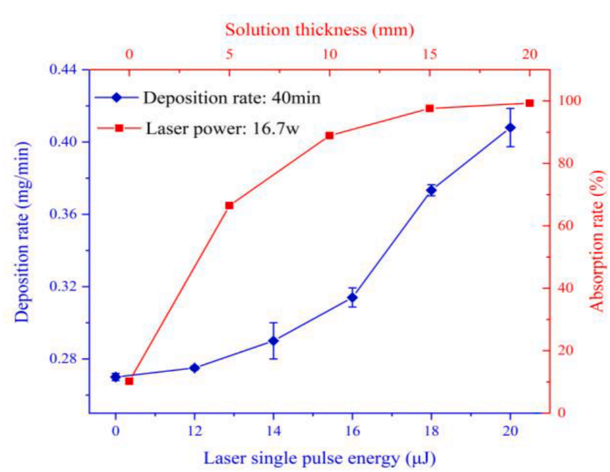

Fig. 2. The influence of different laser single pulse energy on deposition rate and solution absorption rate.

Table 2
Absorption rate of solution for laser power.

Laser power (w)	Empty beaker (w)	Beaker (water)	Beaker (Ni-Fe-P)	Absorption rate (%)
6.74	6.35	5.42	0.29	89.9
9.93	9.22	8.02	0.39	88.9
13.0	12.2	10.7	0.48	90.2
15.9	15.0	12.5	0.57	90.8
17.6	16.2	14.0	0.64	89.4

As shown in Fig. 2, with the increase of laser single pulse energy (12~20μJ), the deposition rate keeps increasing, which is increased about 50% when the laser single pulse energy is 20μJ compared with no laser irradiation.

According to the Nernst equation, the laser thermal effect changes the cathode over-potential and reduces the activation energy required for the ion reaction [17,18], which makes the reduction of ions easier. In addition, the temperature rise in the laser-irradiated area creates a temperature difference with the surrounding solution to form micro-zone stirring, which suppresses concentration polarization and keeps the reaction going [17,18]. The greater the laser single pulse energy, the greater the impact on the cathode over-potential. The greater the temperature difference between the irradiated area and the surrounding solution, the greater the stirring effect of the micro area. Therefore, the deposition rate keeps increasing.

3.2. Degree of amorphousness

As shown in Fig. 3, when the laser single pulse energy is less than 16μJ, the content of P and Ni elements keeps increasing, while the content of Fe decreases. When the laser single pulse energy is greater than 16μJ, the content of Fe element increases, while the content of Ni element decreases and the content of P element does not change much.

The reduction potentials of Ni^{2+} and Fe^{2+} are small and relatively close [13]. In the co-deposition process of Fe and Ni, the deposition of Fe is mainly affected by diffusion, while the deposition of Ni is mainly affected by the activation energy [25,26,27]. Therefore, it is inferred that when the laser single pulse energy is less than 16μJ, the increase in temperature reduces the activation energy of the reaction, making Ni closer to the reduction potential. When the laser single pulse energy is further increased, the degree of influence of activation on Ni reduction becomes smaller while the micro-agitating has a greater impact on the Fe content.

Besides, the content of P element increased at the beginning and then keep steadily. This is because the photoelectric effect generated in the laser irradiated area makes the number of reduced electrons increases. According to the ability of obtaining electrons, the reduction of $H_2PO_2^-$ is the strongest. Therefore, the content of P element increases, indicating amorphous degree becomes larger [3]. However, as the laser single pulse energy further increases, because of the limited $H_2PO_2^-$ in the solution, the P content no longer increases.

As shown in Fig. 4, XRD patterns show that the shape peak at a position of about 45° around 2θ, which is a typical amorphous pattern [3]. In addition, there are several other diffraction peaks, which can be determined as Cu and Cu oxides by comparison with standard cards. The diffraction intensity becomes smaller as the laser single pulse energy increases, indicating that amorphous degree becomes larger. When the laser single pulse energy is 16~20μJ, the diffraction intensity of the coating is not much different, which is consistent with the change of P content.

There are two conditions for the formation of the amorphous state: one is to form small and numerous crystal nuclei, the other is that the cathode hydrogen evolution disrupts the regular arrangement of atoms [3]. Therefore, on the one hand, the laser thermal effect can increase the deposition rate, which is beneficial for the formation of numerous crystal nuclei [17,18,28]. On the other hand, the laser thermal effect can accelerate hydrogen evolution and remove the bubbles in time by micro-area agitation [17,18], which is conducive to the irregular arrangement of atoms and ensure the density of the coating.

3.3. Residual internal stress

The residual internal stress of amorphous Ni-Fe-P alloy is generated due to unbalanced nucleation and non-directional growth in the process of electrodeposition [3], which is difficult to solve the problem by adjusting the parameters of electrodeposition alone.

As shown in Fig. 5, when the laser single pulse energy is less than 16μJ, the residual stress of the coating has been decreasing, reaches 97 Mpa in the form of tensile stress. This is because, on the one hand, part of

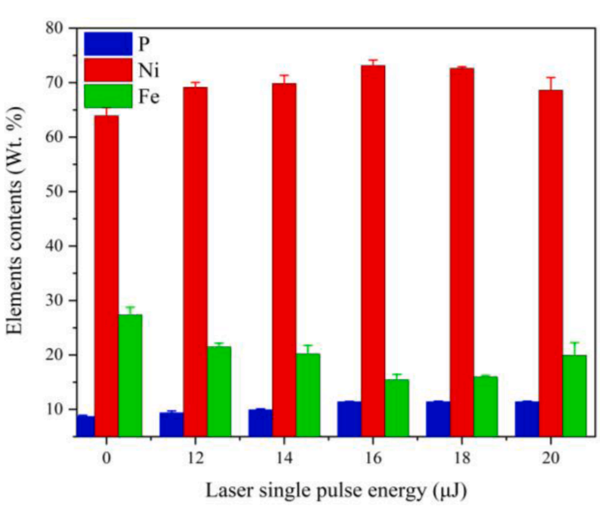

Fig. 3. The influence of different laser single pulse energy on elements contents.

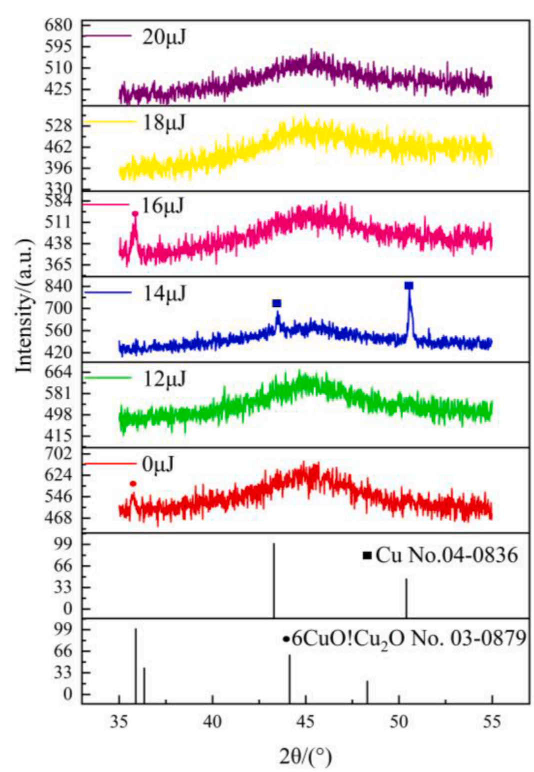

Fig. 4. The XRD patterns of different laser single pulse energy.

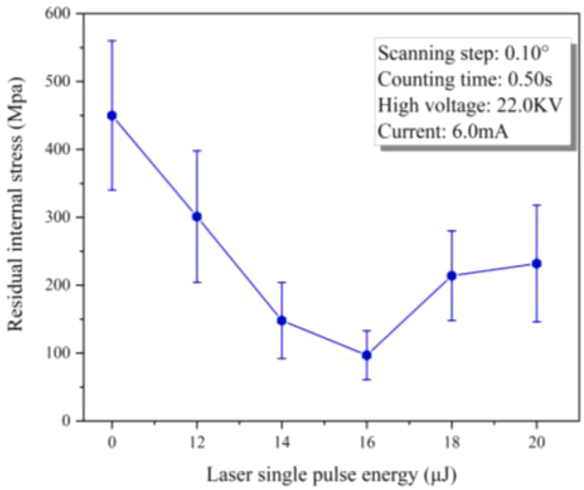

Fig. 5. The influence of different laser single pulse energy on residual internal stress.

the heat of the laser is absorbed by the reducing ions and deposited on the substrate in the form of compressive stress, which can offset part of the tensile stress [17]. On the other hand, when the laser hits the surface of the cathode substrate, there is a downward force impact, which also can offset part of the tensile stress.

However, when the laser single pulse energy is greater than 16μJ, the tensile stress increases again. According to the experimental phenomenon, this may be because when the laser single pulse energy is too large, the hydrogen evolution at the cathode increases. The impact of the laser force and micro-agitating action are difficult to break away the bubbles in time, which weakens the effect of the laser because of refraction and reflection. In addition, during the Fe-Ni co-deposition process, the increase of Fe content will lead to the increase of coating stress [3]. However, when the laser single pulse energy is 16~20μJ, the residual stress and the content of Fe element of the coating is still less than that without laser deposition.

As shown in Fig. 6, when the laser single pulse energy is 12~16μJ, the number and visibility of cracks on the coating surface gradually decrease, which is consistent with the change of residual internal stress. As shown in Fig. 6(a), in the case of single electrodeposition, there are many pores on the surface and the crack density in different parts is not uniform. In addition, there are many white impurities on the surface. Fig. 6(b)~6(c) also have more pores, protrusions and defects on the

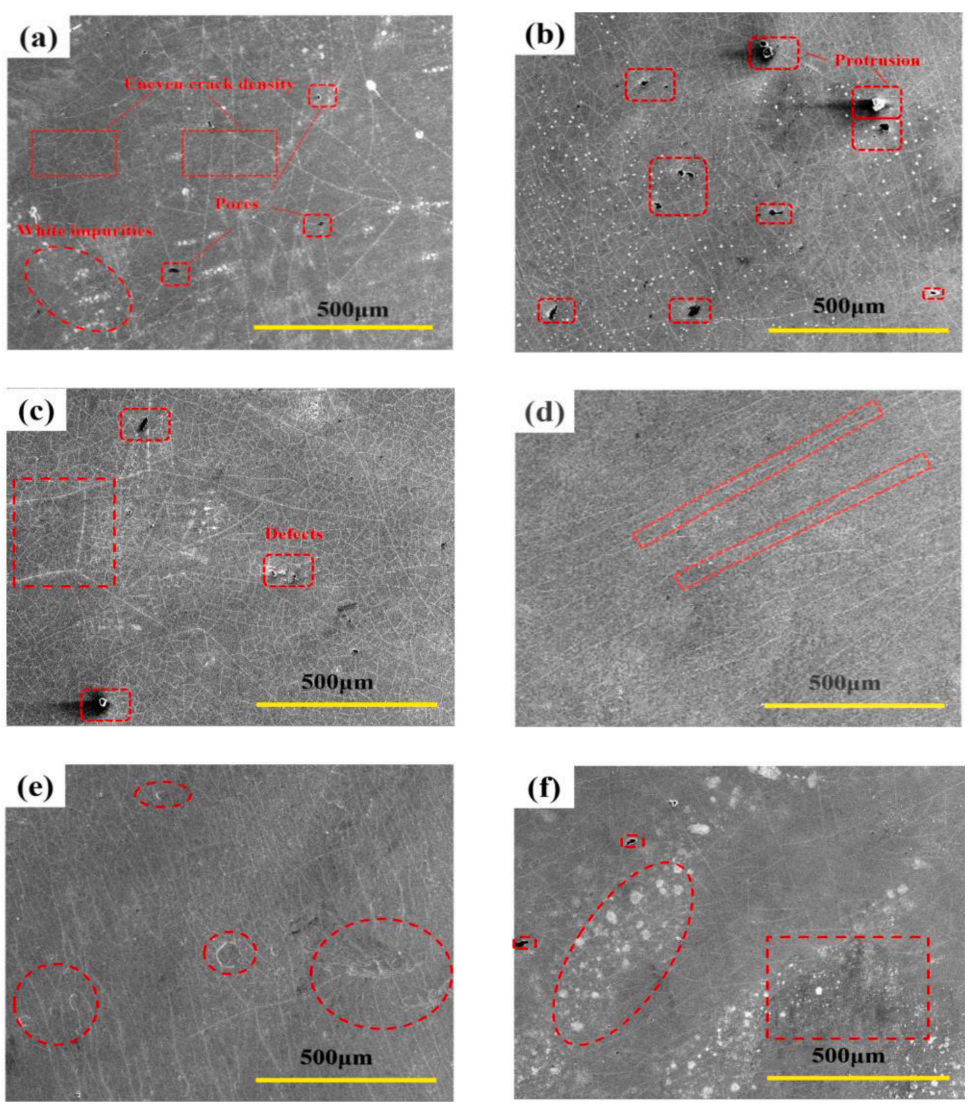

Fig. 6. The influence of different laser single pulse energy on surface morphology (a-0μJ; b-12μJ; c-14μJ; d-16μJ; e-18μJ; f-20μJ;).

surface. In Fig. 6(c), the long cracks on the surface are divided into small areas with a higher density of micro-cracks. However, when the laser single pulse energy is 16μJ, the number of surface cracks is relatively small and the density is uniform. The surface is relatively smooth and flat. This is because, on the one hand, the micro-agitating formed by the laser can take away the bubbles in time, which is also attributed to increase the number of micro-cracks [26]. In addition, the laser irradiation can increase the limiting current density to make the coating denser and smoother [28]. However, when the laser single pulse energy is larger, the surface quality becomes worse and many white impurities appeared according to Fig. 6(f). The absorption rate of the solution to the laser heat can reach 90%. When the laser single pulse energy is too large, on the one hand, the thermal effect increases, which makes the cathode hydrogen evolution phenomenon worse. When there are too many bubbles, gathering on the solution surface, the impact force of laser irradiation is difficult to flush the bubbles in time, which also causes the pores and hydrogen content of the coating to increase. On the other hand, when the laser single pulse energy reaches the breakdown threshold of the solution, cavities will be generated, which causes laser refraction and reflection and leads to the weakening or uneven effect of laser, thus affecting the deposition quality of the coating. As shown in Fig. 6(e), the surface of the deposited layer is uneven. In addition, the occurrence of white spots may be P precipitates [3], due to the uneven laser action.

3.4. Corrosion resistance

It can be seen from Fig. 7 that when the laser single pulse energy is about 16μJ, the loss weight in the 3.5% NaCl and 2mol/L HCl solution is the smallest, indicating that the coating has the best corrosion resistance. In different corrosive solutions, the performance of corrosion resistance is consistent, indicating that our experiment is reliable.

There are many factors that affect the corrosion resistance of amorphous Ni-Fe-P alloys, including amorphous structure, chemical composition and surface quality. Firstly, the atomic arrangement of the amorphous Ni-Fe-P alloy structure is long-range and disordered, which is a uniform single-phase system without defects such as grain boundaries and segregation of chemical components, so intergranular corrosion and stress corrosion will not occur [3]. In addition, the amorphous Ni-Fe-P alloy is a solid solution formed by a variety of elements and its microscopic uniformity and chemical composition can reduce the corrosion of the electrodeposited layer in the corrosive medium [3]. In the corrosion solution, a phosphide film that acts as a passivation film can be formed on the surface of the alloy. During the corrosion process, Fe and Ni are preferentially dissolved. When the content of P element in the coating is higher, a hydrolysis reaction will occur to generate more

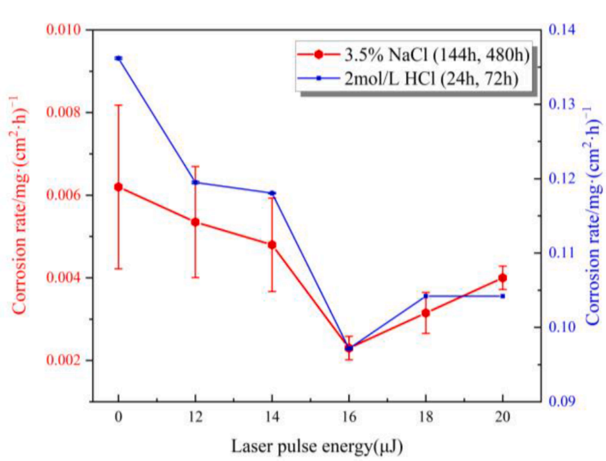

Fig. 7. The influence of different laser single pulse energy on corrosion resistance.

$H_2PO_2^-$, which has a strong reducing ability to reduce Ni^{2+} and Fe^{2+} to Ni and Fe, which is equivalent for chemical passivation. In addition, when there are many defects, such as pores and micro-cracks in Fig. 6(a), the corrosion resistance is poor. The high density of crevices as well as the long micro-cracks in the coating can provide corrosion routs and result in the enhancement of corrosion [26]. In addition, micro-cracks in the monolithic coating conduct the corrosive species to the substrate-coating interface. The presence of corrosion products induces high stresses in the interface and stimulates spallation of the coatings as shown in Fig. 8(a) [26]. According to Fig. 6(d), the surface quality is the best and the number of cracks is the least. When the laser single pulse energy is 16μJ, the corrosion resistance of the coating is the best. As shown in Fig. 8(b), the substrate is still not corroded.

3.5. Hardness and wear resistance

As shown in Fig. 9, as the laser single pulse energy (12~20μJ) increases, the hardness increases at the beginning (12~16μJ) and then (16~20μJ) decreases, which is mainly affected by the element content and the coating structure [3]. Theoretically, the hardness becomes worse with the Fe content decreases when the laser single pulse energy is 12~16μJ [3], however, compact structure can improve hardness and wear resistance. The nucleus size of electrodeposited amorphous alloy is below 2nm [3]. The increase in the deposition rate makes the crystal grains finer [25,29,30] and the diffraction pattern also shows that the crystal structure of the coating becomes less. It is inferred that under laser irradiation, the influence of coating structure on hardness exceeds the influence of element content.

In order to better explain this inference, the coating was tested for wear resistance. As shown in Fig. 9, the coating loses the least quality when the laser single pulse energy is 16μJ, indicating that the wear resistance is the best. Earlier investigators have concluded that hardness of the coating is the most important parameter, which determines the weight loss [30]. Similarly, as the laser single pulse energy (12~20μJ) increases, the wear resistance increases at the beginning (12~16μJ) and then (16~20μJ) decreases.

The surface quality has the greatest impact on the wear resistance. According to the surface morphology in Fig. 6(a)~(f), it is consistent with the displayed wear resistance. When the cracks are more obvious and the surface defects are more, the wear resistance is worse. For amorphous Ni-Fe-P alloys, the greater the degree of the amorphous state, the worse the wear resistance [3]. However, when the laser single pulse energy is 12~16μJ, the degree of amorphous state of Ni-Fe-P increases and the content of Fe element decreases, the wear resistance will decrease [3,27,31], but the results is opposite. Therefore, it can be considered that surface quality is the main factor affecting wear resistance because of grain refinement and hardness by laser irradiation.

Fig. 10 is the friction coefficient curve of the coating with different laser single pulse energy. As it is apparent, initially the coefficient of friction has suddenly increased and after a maximum decreased and then in most cases reached to a steady state [27]. However, when there is no laser irradiation, after the action time exceeds 500s, the coefficient of friction has an obvious downward inflection point, which can be considered as the surface state of the coating has been destroyed according to Fig. 11(a) because of high stress at the contact region [32]. When the laser single pulse energy is 12μJ, the similar change process is also insignificant due to the laser effect. When the laser energy further increases (16μJ), the downward trend of the friction curve is delayed and the time of the inflection point moves later, indicating that the coating has better wear resistance, which is that because of lower stress in the contact area, as well as improved grain refinement and hardness [17,18,32].

Compare the coating morphology after abrasion with or without laser irradiation (16μJ), as shown in Fig. 11. The surface is severely detached and the width of the wear trace reaches 746μm without laser irradiation in Fig. 11(a). However, the wear trace is relatively narrow,

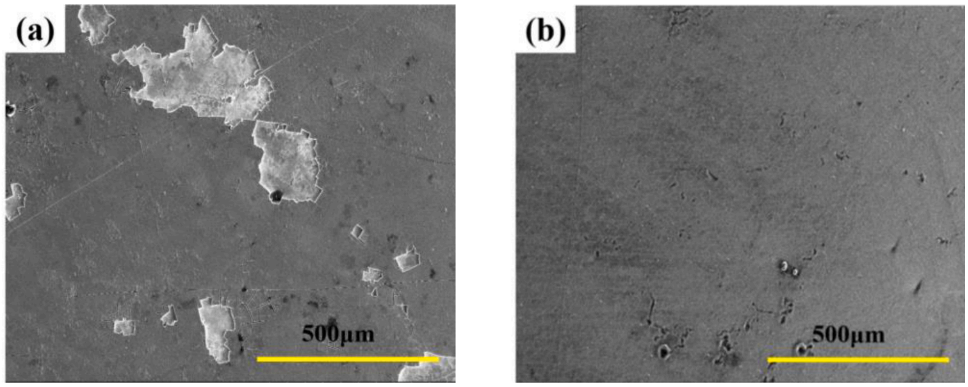

Fig. 8. Surface morphology of the corroded coating (3.5% NaCl, a-No laser, b-16μJ).

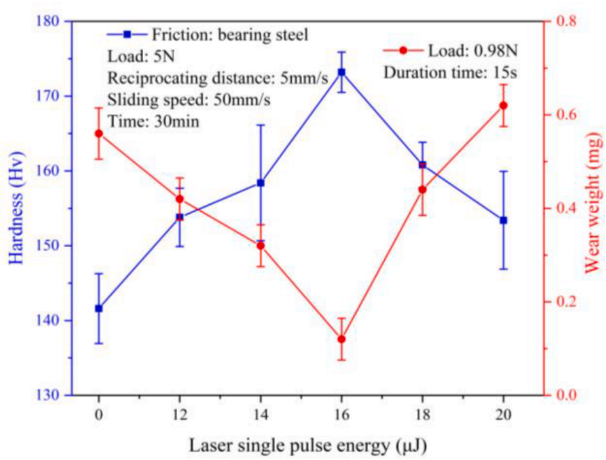

Fig. 9. The influence of different laser single pulse energy on hardness and wear resistance.

only 342μm and the depth is relatively shallow with laser irradiation (16μJ) in Fig. 11(b), indicating that the coating prepared after introducing the laser has better wear resistance. According to the wear surface in Fig. 11(a), the material has been removed on both sides of the wear scar and plastic deformation has occurred [33]. However, the wear surface of Fig. 11(b) shows relatively slight friction marks, indicating the effect of abrasive on the surface [33]. In addition, according to Fig. 11 (a), it is found that the base of the layer is indeed exposed, which proves the interpretation of the friction coefficient curve.

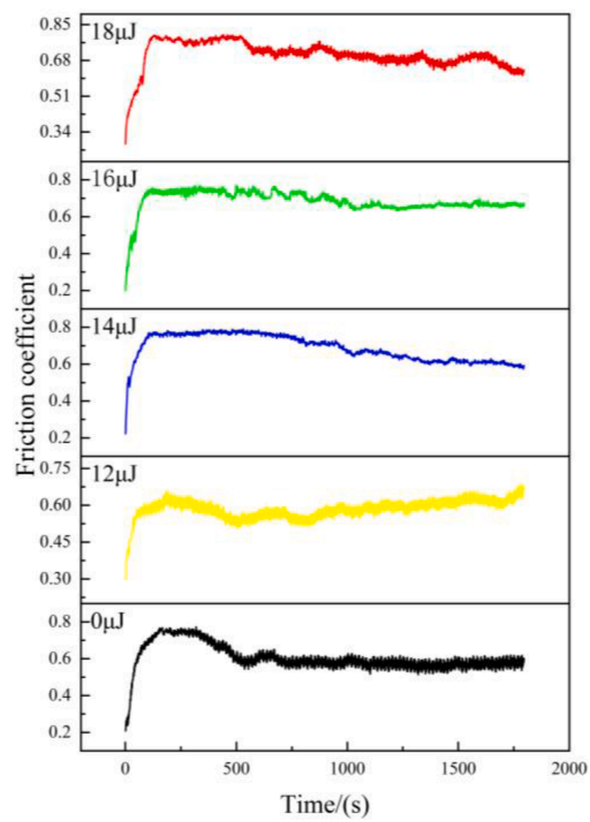

Fig. 10. The influence of different laser single pulse energy on friction coefficient.

4. Conclusions

In this study, amorphous Ni-Fe-P alloy was prepared by constructing a laser-assisted electrodeposition system. The influence of laser irradiation on deposition rate, residual internal stress, surface morphology, degree of amorphousness and coating performance was discussed.

Laser irradiation increases the deposition rate of amorphous Ni-Fe-P alloy about 50% compared with no laser irradiation when the laser single pulse energy is 20μJ. Because laser irradiation can reduce the activation energy required for ion reduction and the irradiated area forms micro-agitated areas to suppress concentration polarization.

Laser irradiation reduces the residual tensile stress of the amorphous Ni-Fe-P alloy, reaching 97 Mpa when the laser single pulse energy is 16μJ. The joint action including the force impact of the laser on the deposited layer and the absorption of some heat by the reducing ions offsets part of the tensile stress. Laser irradiation reduces the number of cracks and improves the finish of the coating. The surface quality is optimal when the laser single pulse energy is 16μJ.

Laser irradiation affects the content of Fe and Ni in the amorphous Ni-Fe-P alloy due to the laser effect on the activation energy and micro-zone stirring. The photoelectric effect produced by laser irradiation increases the content of P element, thereby increasing the degree of amorphousness of the coating.

The impact of the laser irradiation for the structure is greater than the effect of the element on the coating performance. Amorphous Ni-Fe-P alloy has the best corrosion resistance, hardness and wear resistance when the laser single pulse energy is 16μJ.

Credit authorship contribution statement

Yucheng Wu: Conceptualization, data curation, investigation, methodology, roles/writing-original draft, writing-review&editing. **Zhaoyang Zhang:** Funding acquisition, resources, supervision, project

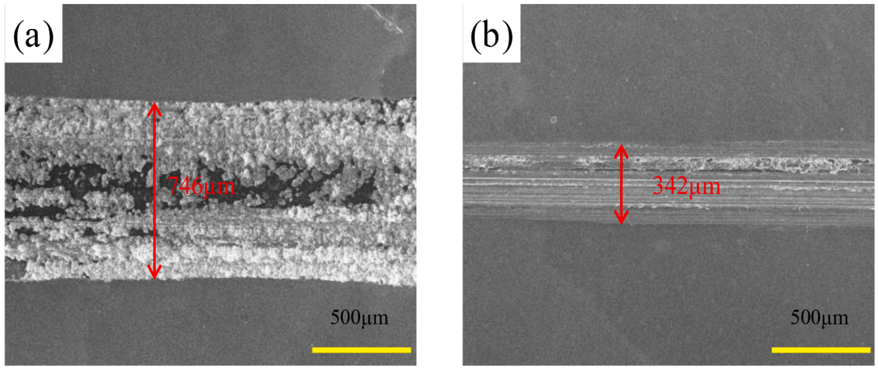

Fig. 11. Surface morphology after abrasion with or without laser irradiation (a-0μJ; b-16μJ).

administration, validation, writing-review&editing. **Kun Xu:** Funding acquisition, investigation. **Jinzhong Lu:** investigation, resources. **Xueren Dai:** Data curation, formal analysis. **Hao Zhu:** Funding acquisition, investigation. **Shuai Yang:**Investigation, data curation.

Declaration of Competing Interest

The authors declare that they have no known competing financial interests or personal relationships that could have appeared to influence the work reported in this paper.

Acknowledgement

The authors would like to thank the support of National Natural Science Foundation of China (Grant No.52075227), Natural Science Foundation of Jiangsu Province (Grant No. BK20180873, No. BK20180875).

References

[1] J.Q. Lian, Y.H. Wu, H.A. Zhang, S.Y. Gu, Z.W. Zeng, X.Y. Ye, One-step synthesis of amorphous Ni-Fe-P alloy as bifunctional electrocatalyst for overall water splitting in alkaline medium, Int. J. Hydrog. Energy. 43 (2018) 12929–12938. https://doi.org/10.1016/j.ijhydene.2018.05.107.
[2] Z.T. An, X.Y. Zhang, H.G. Li, A preliminary study of the preparation and characterization of shielding fabric coated by electrical deposition of amorphous Ni-Fe-P alloy, J. Alloy. Compd. 621 (2015) 99–103. https://doi.org/10.1016/j.jallcom.2014.09.163.
[3] Z.M. Tu, M.Z. An, H.L. Hu, Modern Theory and Technology of Alloy Electrodeposition, National Defense Industry Press, Beijing, 2016.
[4] L. Liu, J. Peng, X.M. Du, H. Zheng, Z.W. Chen, P. Gong, Y. Xiao, X.Q. Cao, Synthesis, composition, morphology, and wettability of electroless Ni-Fe-P coatings with varying microstructures, Thin Solid Films 706 (2020), 138080. https://doi.org/10.1016/j.tsf.2020.138080.
[5] T. Falcade, V. Turq, J.P. Bonino, C.F. Malfatti, Tribological properties of amorphous carbon films obtained by electrodeposition from DMF using 2HEAL protic ionic liquid as dopant, Diam. Relat. Mater. 71 (2017) 30–37. https://doi.org/10.1016/j.diamond.2016.11.014.
[6] C.H. Gao, Stability of electrodeposited amorphous Ni-Fe-P alloys, Trans. Nonferrous Met. Soc. China. 16 (2006) 1325–1330. https://doi.org/10.1016/S1003-6326(07)60014-4.
[7] V.V. Ursaki, V. Lair, L. Živković, M. Cassir, A. Ringuedé, O. Lupan, Optical properties of Sm-doped ceria nanostructured films grown by electrodeposition at low temperature, Opt. Mater. 34 (2012) 1897–1901. https://doi.org/10.1016/j.optmat.2012.05.026.
[8] Nitin P. Wasekar, Neha Hebalkar, A. Jyothirmayi, B. Lavakumar, M. Ramakrishna, G. Sundararajan, Influence of pulse parameters on the mechanical properties and electrochemical corrosion behavior of electrodeposited Ni-W alloy coatings with high tungsten content, Corrosion Sci 165 (2020), 108409. https://doi.org/10.1016/j.corsci.2019.108409.
[9] C.A. Vlaic, M. Kurniawan, R. Peipmann, C.C. Lalău, M. Stich, U. Schmidt, A. Bund, Improved wear resistance of alternating amorphous and crystalline layers in electrodeposited Ni-P multilayers, Surf. Coat. Technol. 386 (2020), 125470. https://doi.org/10.1016/j.surfcoat.2020.125470.
[10] E. Bertero, M. Hasegawa, S. Staubli, E. Pellicer, I.K. Herrmann, J. Sort, J. Michler, L. Philippe, Electrodeposition of amorphous Fe-Cr-Ni stainless steel alloy with high corrosion resistance, low cytotoxicity and soft magnetic properties, Surf. Coat. Technol. 349 (2018) 745–751. https://doi.org/10.1016/j.surfcoat.2018.06.003.
[11] B.S. Li, A. Lin, X. Wu, Y.M. Zhang, F.X. Gan, Electrodeposition and characterization of Fe-Cr-P amorphous alloys from trivalent chromium sulfate electrolyte, J. Alloy. Compd. 453 (2008) 93–101. https://doi.org/10.1016/j.jallcom.2006.11.162.
[12] L. Sziráki, E. Kuzmann, G.B. Lak, M. El-Sharif, C.U. Chisholm, S. Stichleutner, K. Havancsák, K. Zih-Perényi, Z. Homonnay, A. Vértes, Study of electrodeposition of amorphous Sn-Ni-Fe ternary alloys from a gluconate-based electrolyte, Surf. Coat. Technol. 211 (2012) 184–187. https://doi.org/10.1016/j.surfcoat.2011.09.024.
[13] Y. Chen, Modern Practical Electroplating Technology, National Defence Industry Press, Beijing, 2003.
[14] A. Karimzadeh, M. Aliofkhazraei, F.C. Walsh, A review of electrodeposited Ni-Co alloy and composite coatings: Microstructure, properties and applications, Surf. Coat. Technol. 372 (2019) 463–498. https://doi.org/10.1016/j.surfcoat.2019.04.079.
[15] W. Khalfaoui, E. Valerio, J.E. Masse, M. Autric, Excimer laser treatment of ZE41 magnesium alloy for corrosion resistance and microhardness improvement, Opt. Laser. Eng. 48 (2010) 926–931. https://doi.org/10.1016/j.optlaseng.2010.03.009.
[16] G.R. Gordani, R.S. Razavi, S.H. Hashemi, A.R.N. Isfahani, Laser surface alloying of an electroless Ni-P coating with Al-356 substrate, Opt. Laser. Eng. 46 (2008) 550–557. https://doi.org/10.1016/j.optlaseng.2008.02.002.
[17] Z.Y. Zhang, Y.J. Jiang, L. Huang, X. Nie, G. Liu, Experiment study of laser thermal enhanced electrochemical deposition, Microsyst. Technol. 23 (2017) 1695–1701. https://doi.org/10.1007/s00542-015-2759-1.
[18] X.R. Dai, Z.Y. Zhang, Y.J. Jiang, J. Jiao, W. Jiang, Effects of Laser Irradiation on a Copper Electrodeposition Process and Coating Quality, Int. J. Electrochem. Sci. 12 (2017) 9747–9757. https://doi.org/10.20964/2017.10.73.
[19] Z.L. Yu, X.D. Meng, M. Yin, M. Sun, M. Yuan, H.B. Li, Pulsed laser-assisted ionic liquid electrodeposition of gallium nanoparticles and germanium nanostructures for energy storage, Chem. Phys. Lett. 698 (2018) 181–186. https://doi.org/10.1016/j.cplett.2018.03.023.
[20] Z.L. Yu, X.D. Meng, Y. Hu, M. Yin, P.X. Yang, H.B Li, Pulsed laser irradiation-assisted electrodeposition of germanium in ionic liquid: From amorphous film to polycrystalline branched structures, Mater. Res. Bull. 93 (2017) 208–213. https://doi.org/10.1016/j.materresbull.2017.05.008.
[21] C.H. Cho, H.S. Shin, C.N. Chua, Selective electrodeposition of copper on stainless steel using laser irradiation, Surf. Coat. Technol. 222 (2013) 15–24. https://doi.org/10.1016/j.surfcoat.2013.01.046.
[22] J. Ramiro, A. Perea, J. FTrigo, Y. Laazizc, E.G. Camarero, Pulsed laser deposition and electrodeposition techniques in growing CdTe and $Cd_xHg_{1-x}Te$ thin films, Thin Solid Films 361-362 (2000) 65–69. https://doi.org/10.1016/S0040-6090(99)00770-1.
[23] S.Y. Jin, A. Ziabari, Y.R. Koh, M. Saei, X.M. Wang, B.W. Deng, Y.W. Hu, Je H. Bahk, A. Shakouri, G.J. Cheng, Enhanced thermoelectric performance of P-type $Bi_xSb_{2-x}Te_3$ nanowires with pulsed laser assisted electrochemical deposition, Extreme. Mech. Lett. 9 (2016) 386–396. https://doi.org/10.1016/j.eml.2016.04.010.
[24] I. Zouari, A. Bellagi, F. Lapicque, Thermal effects of a laser beam on the electrodeposition of Ni-P alloys, J. Appl. Electrochem. 28 (1998) 80–88. https://doi.org/10.1023/A:1003253903124.
[25] V. Torabinejad, M. Aliofkhazraei, S. Assareh, M.H. Allahyarzadeh, A. Sabour Rouhaghdam, Electrodeposition of Ni-Fe alloys, composites, and nano coatings-A review, J. Alloy. Compd. 691 (2017) 841–859. https://doi.org/10.1016/j.jallcom.2016.08.329.
[26] V. Torabinejad, M. Aliofkhazraei, A.S. Rouhaghdam, M.H. Allahyarzadeh, Corrosion properties of Ni-Fe-Cr (III) multilayer coating synthesized via pulse duty cycle variation, Mater. Corros. 68 (2017) 347–354. https://doi.org/10.1002/maco.201609071.
[27] V. Torabinejad, A.S. Rouhaghdam, M. Aliofkhazraei, M.H. Allahyarzadeh, Electrodeposition of Ni-Fe and Ni-Fe-(nano Al2O3) multilayer coatings, J. Alloy. Compd. 657 (2016) 526–536. https://doi.org/10.1016/j.jallcom.2015.10.154.
[28] V. Torabinejad, M. Aliofkhazraei, A.S. Rouhaghdam, M.H. Allahyarzadeh, The hydrophobicity of Ni-Fe alloy electrodeposits obtained at different current densities, Trans. Inst. Metal Finish. 60 (2017) 923–931. https://doi.org/10.1080/00202967.2017.1323622.

[29] Q.L. Xiao, S.Y. Shao, J.D. Shao, X.Z. Fan, Influences of Oxygen Partial Pressure and Deposition Rate on Residual Stress of YSZ Thin Films, Chin. J. Lasers. 36 (2009) 1195–1199. https://doi.org/10.3788/CJL20093605.1195.
[30] V. Torabinejad, M. Aliofkhazraei, A. S. Rouhaghdam, M. H. Allahyarzadeh, T. Kasama, H. Alimadadi. Mechanical properties of multilayer Ni-Fe and Ni-Fe-Al2O3 nanocomposite coating. Mater. Sci. Eng. A. https://doi.org/10.1016/j.msea.2017.06.009.
[31] V. Torabinejad, M. Aliofkhazraei, A.S. Rouhaghdam, M.H. Allahyarzadeh, Tribological performance of Ni-Fe-Al_2O_3 multilayer coatings deposited by pulse electrodeposition, Wear 380-381 (2017) 115–125. https://doi.org/10.1016/j.wear.2017.03.013.
[32] V. Torabinejad, M. Aliofkhazraei, A.S. Rouhaghdam, M.H. Allahyarzadeh, Tribological Behavior of Electrodeposited Ni-Fe Multilayer Coating, Tribol. Trans. 60 (2017) 923–931. https://doi.org/10.1080/10402004.2016.1230687.
[33] V. Torabinejad, M. Aliofkhazraei, A.S. Rouhaghdam, M.H. Allahyarzadeh, Tribological properties of Ni-Fe-Co multilayer coatings fabricated by pulse electrodeposition, Tribol. Int. 106 (2017) 34–40. https://doi.org/10.1016/j.triboint.2016.10.025.